*Proceedings of the*
*Annual Stability Conference*
*Structural Stability Research Council*
*San Antonio, Texas, March 19-22, 2024*

# Experimental studies on the stability of aluminum sections and beam-columns

Prachi Verma[1], Sahar Dahboul[2], Liya Li[3], Pampa Dey[4], Nicolas Boissonnade[5]

## Abstract
Extruded aluminum members are known to be more prone to buckling than carbon steel members, owing to a lower Young's modulus that is one-third that of steel. Further, their pronounced non-linear material response and associated strain hardening effects have a non-negligible influence on their stability response. This paper therefore presents the results of an experimental test series on extruded 6061-T6 aluminum sections and beam-columns. Typical tensile tests and careful measurements of both local and global imperfections were achieved and are reported. Four sections under pure compression and two beam-columns under eccentric compression were tested to study the buckling behavior of extruded aluminum I and H profiles. Comparisons with code resistance predictions from the Canadian Standards CSA S157 reveal a significant potential for improvements, and corresponding indications for a more accurate stability design of aluminum members.

## 1. Introduction
Aluminum (Al) offers various advantages as a construction material such as a high strength to weight ratio, good corrosion resistance, ease of fabrication, aesthetical appearance, low maintenance costs, etc. (Beaulieu and Marsh, 2006). Despite these multiple advantages, the use of structural aluminum still remains limited in the construction industry. This is because aluminum members when used in structures suffer from buckling instabilities when subjected to compression and/or flexure. Therefore, aluminum typically stands as a secondary choice after carbon-steel, the latter being less prone to buckling owing to its higher elastic modulus (nearly three times higher). However, the stability issues of Al members can be improved by increasing the stiffness of the cross-sections considered. Higher stiffness can be achieved by using hollow cross-sections, complex cross-sections or even (stiffened) open cross-sections that yield higher moments of inertia. In this regard, current design standards, such as the Canadian Standard CSA S157 (Canadian Standards Association, 2017), Eurocode 9 (European Committee for Standardization, 2007) and the American Standard – Aluminum Design Manual (ADM) (Aluminum Association, 2020), provide buckling design provisions which are applicable to simple cross-sections of regular geometry such as I, H, rectangular hollow, square hollow sections, etc. However, the resistance

[1] PhD student, Laval University, <prachi.verma.1@ ulaval.ca >
[2] PhD student, Laval University, <sahar.dahboul.1@ulaval.ca>
[3] Assistant Professor, Sherbrooke University, <liya.li@usherbrooke.ca>
[4] Assistant Professor, Laval University, <pampa.dey@gci.ulaval.ca>
[5] Full Professor, Laval University, <nicolas.boissonnade@gci.ulaval.ca>

predictions calculated as per these standards are usually not accurate – they are often quite conservative. For example, various studies on different aluminum cross-section profiles such as angles, I-shapes, stiffened closed sections, H and rectangular hollow sections, have shown that current design standards predict conservative resistance values (Liu et al., 2015) (Yuan et al., 2022). Yet, on the other hand, some other research works have shown that current standards sometimes overestimate resistance values. For example, (Wang et al., 2016) from their investigation on large sections of extruded Al alloy I and rectangular hollow sections (RHSs) found that although Eurocode 9 and Chinese Code GB 50429 predict conservative resistance values, the American Aluminum Design Manual may overestimate resistance values. Similarly, (Zhang et al., 2020) found that current design provisions yield unsafe and scattered predictions for pin-ended unequal angle columns.

Therefore, there is a need for extensive research in this area to study the buckling phenomenon experimentally and numerically, so as to come up with better resistance predictions of aluminum members, which shall lead to improve economy in structural design and at the same time ensuring safety and accuracy. In this study, experimental investigations have been performed on four short compact sections and two relatively long beam columns under pure compression and eccentric compression, respectively. In addition, tensile coupon tests and careful geometric initial imperfection measurements have also been performed in order to obtain accurate material and geometric properties. Finally, the suitability of Canadian Standard CSA S157 is investigated by comparing peak loads obtained from experimental testing to the resistance predicted by the Canadian Standard.

## 2. Description of specimens

This study comprises performing experimental tests on extruded 6061-T6 aluminum short specimens and relatively long members of I and H cross-section profiles as shown in Fig. 1. The nominal geometric dimensions and length for each of these specimens are provided in Table 1, where $b$ and $h$ stand for the width and height of flange and web, respectively, while $t$ and $f_y$ stand for thickness and yield strength, respectively.

A total of 4 simple compression tests and 2 eccentric compression tests were conducted on short members and relatively long members, respectively. For brevity, in the following text short specimens will be abbreviated simply as ‘sections’ and relatively long members as ‘members’.

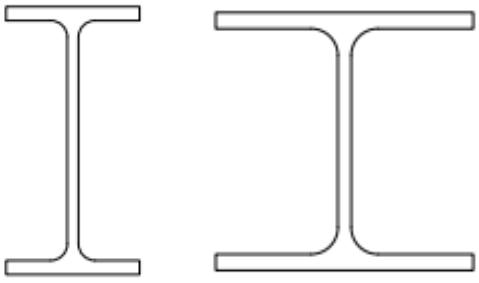

(a) (b)

Figure 1: Cross-section profiles considered in this study: (a) I-cross-section; (b) H cross-section

Table 1: Nominal dimensions of specimens

| Specimen | $b_{flange}$ [mm] | $t_{flange}$ [mm] | $h_{web}$ [mm] | $t_{web}$ [mm] | $f_y$ [MPa] | $L$ [mm] |
|---|---|---|---|---|---|---|
| Sections | | | | | | |
| I6x3.92-1 | 76.2 | 7.92 | 152.4 | 6.35 | 240 | 400 |
| I6x3.92-2 | 76.2 | 7.92 | 152.4 | 6.35 | 240 | 400 |
| WF6x7.61-1 | 152.4 | 9.53 | 152.4 | 7.92 | 240 | 400 |
| WF6x7.61-2 | 152.4 | 9.53 | 152.4 | 7.92 | 240 | 400 |
| Members | | | | | | |
| WF6x7.61-3 | 152.4 | 9.53 | 152.4 | 7.92 | 240 | 1000 |
| WF6x7.61-4 | 152.4 | 9.53 | 152.4 | 7.92 | 240 | 1500 |

## 3. Preliminary measurements on specimens

Several preliminary measurements such as geometrical imperfections' measurements on the surface of the specimens and measurements of actual yield and ultimate strength of the alloy used using tensile coupon tests have been done in this study. Details of each of these tests are given in the following subsections.

### *3.1 Measurement of geometric imperfections*

Accurate measurement of geometrical imperfections is a crucial step as they significantly affect the buckling capacity of aluminum sections and members. In this study, geometric imperfections for all the specimens have been measured using a 3D scanning technology which involves scanning the specimen surface using a handy MetraScan that is used in coordination with a C-Track device, with the help of VXelements computer software as shown in Fig. 2. This device is capable of measuring imperfection amplitudes up to an accuracy of 0.025 *mm*. Fig. 3 shows the scanned geometry comprising of the mesh of scanned points for I and H sections.

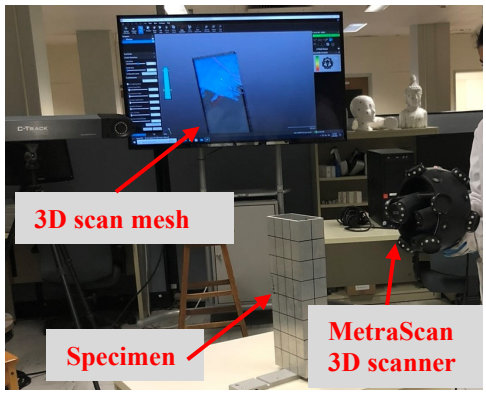

Figure 2: Laser scanning process with MetraScan

The information on the geometrical imperfections is meant at being used later within the validation of F.E.-based numerical shell models in software Abaqus; once validated, the numerical models will be used along parametric studies to further investigate the influence of geometrical imperfections on their buckling behavior, as well as other influences.

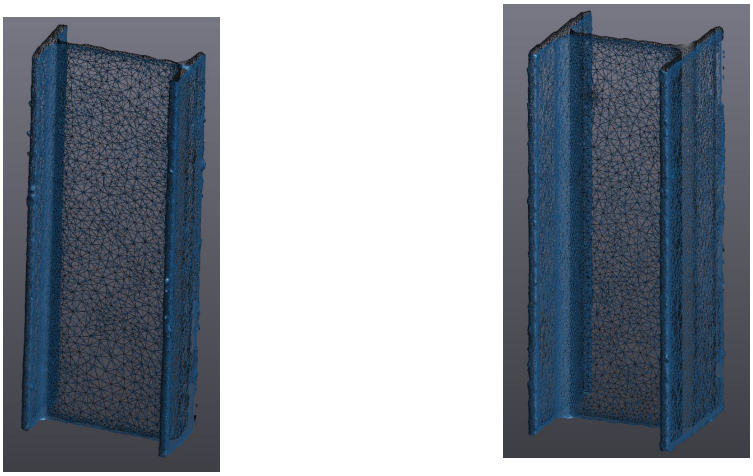

(a) (b)

Figure 3: Scanned geometrical imperfections of cross-sections: (a) I-cross-section; (b) H cross-section

*3.2 Tensile coupon tests*

In order to characterize the actual material behavior of the specimens, especially their stress-strain response, tensile coupon tests are necessary. In this study, 4 tensile coupon specimens were machined, two each for I and H sections, respectively. This repetition of tests was aimed at ensuring the accuracy of the coupon test results. The coupons were manufactured according to the ASTM standard (Testing and Materials, 2015) and to EN ISO 377 standard (European standard,1997) and were cut out from flanges and webs of the specimens. The coupons were tested using a 500 *kN* MTS hydraulic testing machine under displacement-controlled conditions. The testing procedure and loading rate followed the recommended guidelines provided in (Huang and Young, 2014). In this process, the Young's modulus was determined several times to obtain an accurate final value.

Fig. 4 shows the tested coupons and Fig. 5 shows the obtained engineering stress-strain curves for the two I and two H sections, respectively. Table 2 reports on the obtained Young's modulus $E_0$, and yield strength taken as 0.2% proof stress $\sigma_{0.2}$, 1.0 % proof stress $\sigma_{0.1}$ and on the ultimate tensile strength $\sigma_u$ of the tested coupons. Tensile coupon tests for the I and H member specimens are currently underway.


Figure 4: Tested tensile coupons for I and H sections

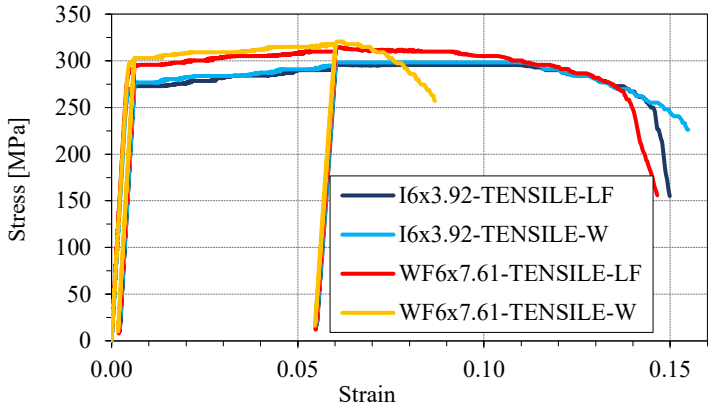


Figure 5: Stress-strain graph for tensile coupon tests

Table 2: Material properties obtained from tensile coupon tests

| Specimen | $E_0$ [MPa] | $\sigma_{0.2}$ [MPa] | $\sigma_{1.0}$ [MPa] | $\sigma_u$ [MPa] |
|---|---|---|---|---|
| I6x3.92-1 | 67527 | 272.14 | 273.49 | 295.49 |
| I6x3.92-2 | 66064 | 276.81 | 278.79 | 298.17 |
| WF6x7.61-1 | 69649 | 295.31 | 296.70 | 314.28 |
| WF6x7.61-2 | 68463 | 303.29 | 306.71 | 320.55 |

## 4. Tests on sections under pure compression

In this study, a total of 4 pure compression tests on sections have been performed (i.e., stub column tests): two identical each for I and H sections to ensure the accuracy and validity of the test results. Fig. 6 shows the experimental setup for these tests. The length of each specimen has been chosen around three times the maximum height of the cross-section in order to avoid any significant influence of flexural or member buckling. Fixed-fixed boundary conditions have been provided at both top and bottom of the specimen, except axial displacement at top plate so as to allow for compression stresses in the specimens. Tests were performed on a 5000 *kN* SATEC testing machine under displacement-controlled conditions and axial displacement, or end shortening, have been measured through a displacement transducer placed at the top of specimen as shown in Fig. 6.

Fig. 7 shows buckling failure modes for all the cross-section specimens, where it can be seen that all specimens have undergone local buckling failure at some point. Also, the failure modes for the identical tests for each of I and H sections are similar, indicating a certain reliability in the testing. Fig. 8 provides typical load-end shortening plots for these tests; it can be seen that the curves from repeated tests almost overlap, again indicating the reliability of tests. Detailed results are reported later in the paper.

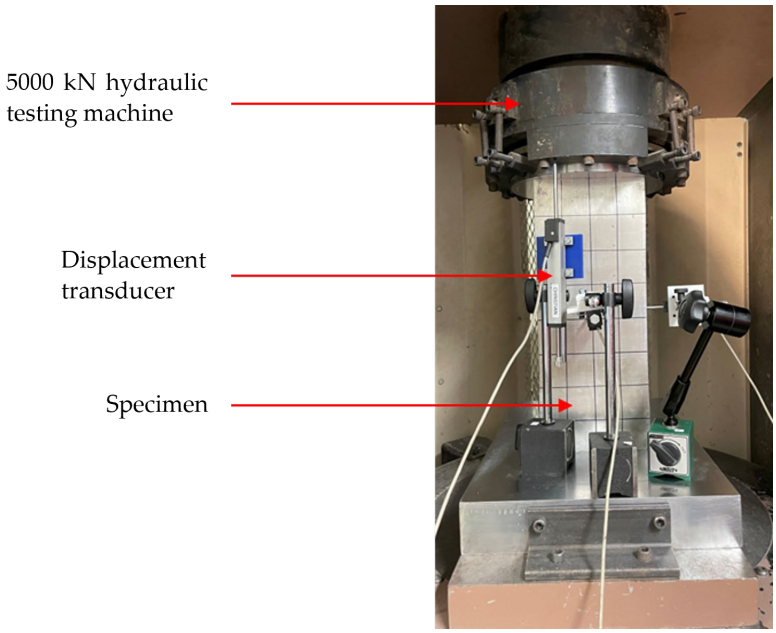


Figure 6: Experimental setup for sections under pure compression

Table 3 in Section 5 presents the peak load attained ($N_{exp}$) and the corresponding displacement for all the specimens from experimental testing, along with comparison of resistance predictions from Canadian Standard CSA S157. It can be observed that resistance predictions from CSA S157 ($N_{CSA\text{-}157}$) are higher than test results by around 25 to 30 % for I and H cross-sections, indicating a conservative nature of the design standards considered. In the next phase of these research investigations, this experimental database will be employed to validate existing design recommendations for predicting the local buckling behavior of aluminum extruded sections as well as validating a non-linear shell F.E. model for such sections.

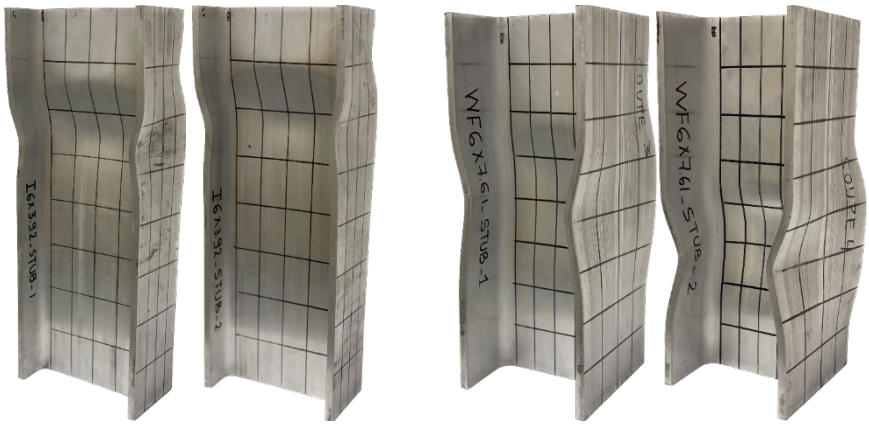

Figure 7: Tested sections under pure compression showing local buckling failure

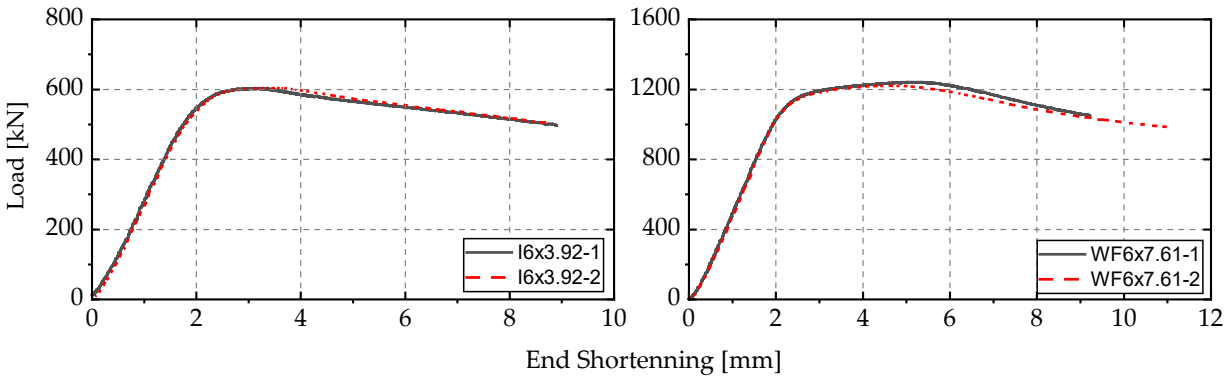

Figure 8: Load-end shortening graphs for tests under pure compression

## 5. Tests on members under eccentric compression

Two moderately slender members of H cross-section with lengths of 1 *m* and 1.5 *m*, respectively, have been tested under eccentric compression. The member of length 1 *m* was tested under compression + biaxial bending, and the member of length 1.5 *m* was tested under compression and uniaxial bending.

The tests were conducted on a 2000 *kN* MTS hydraulic testing machine as shown in Fig. 9. The test setup consisted in two end plates between which the member was placed. These end plates were connected to the member through a hydraulic clamp and two regular clamps. The end supports were equipped with cylindrical rollers acting as hinges that allowed rotation of end plates about the rollers. An eccentricity *e* was set from the axis of the cylindrical roller as shown in the sketch of Fig. 10, leading to compression + mono-axial bending. However, to achieve compression + biaxial bending loading, the member was in addition rotated by an angle $\alpha$ around its longitudinal axis: in this position, the bending moment caused by the application of an eccentric compression results in bending about the two principal axes of the section.

Four displacement transducers (LVDTs) – 2 at top and 2 at bottom end plates – were used to measure the end displacement and rotation of the specimen. Moreover, four 'string displacement transducers' were mounted at mid-height of the member to measure the lateral displacement and torsional twist at mid-height of the beam-column. 2 strain gauges were also attached at the mid-height of the member to record the variation of strain during the loading. The tests were conducted under displacement-controlled loading at the rate of 0.2 *mm*/*minute* and the tests were stopped long after reaching peak loads.

Fig. 11 shows the buckled shape of both the members specimens, i.e., WF6x7.61-3 and WF6x7.61-4, respectively. It can be observed that the member specimens have undergone both global buckling as well as local buckling. Local buckling is very obvious in the flanges and webs of the specimens. Moreover, Fig. 12 and Table 3 show the obtained load-displacement curves and the value of the peak loads and the corresponding displacements for the two member tests, respectively. The member specimen WF6x7.61-3 has attained a higher peak load of 945 *kN* as compared to the peak load of 727 *kN* attained by specimen WF6x7.61-4. This was expected since the former member is less slender (length of 1 *m*) as compared to the latter (length of 1.5 *m*), indicating here again the significant role of slenderness in the capacity of the aluminum members.

In the next phases of these research investigations, this experimental database will be employed to examine the performances of existing design standards for predicting the local and global buckling behavior of aluminum extruded sections and members.

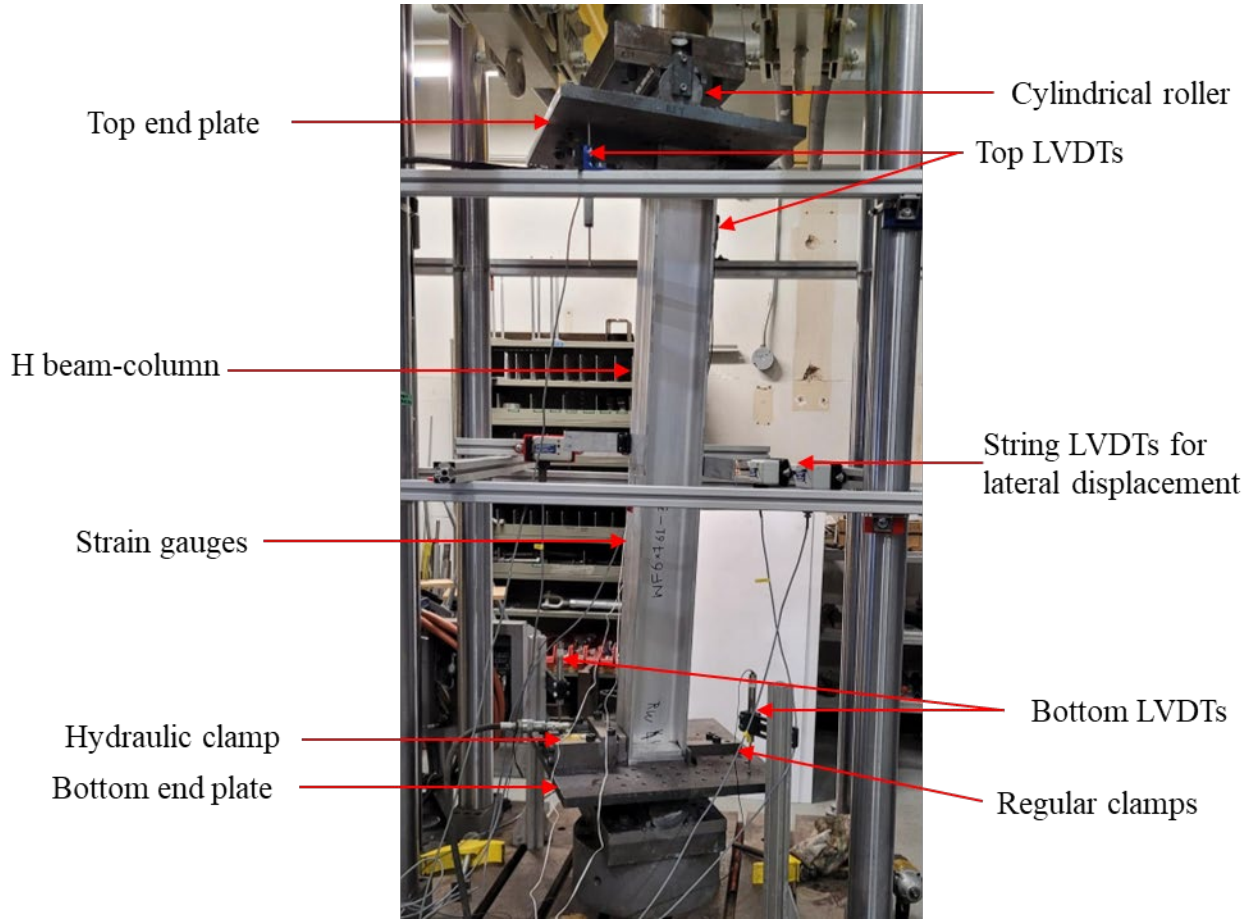


Figure 9: Experimental setup for members under eccentric compression

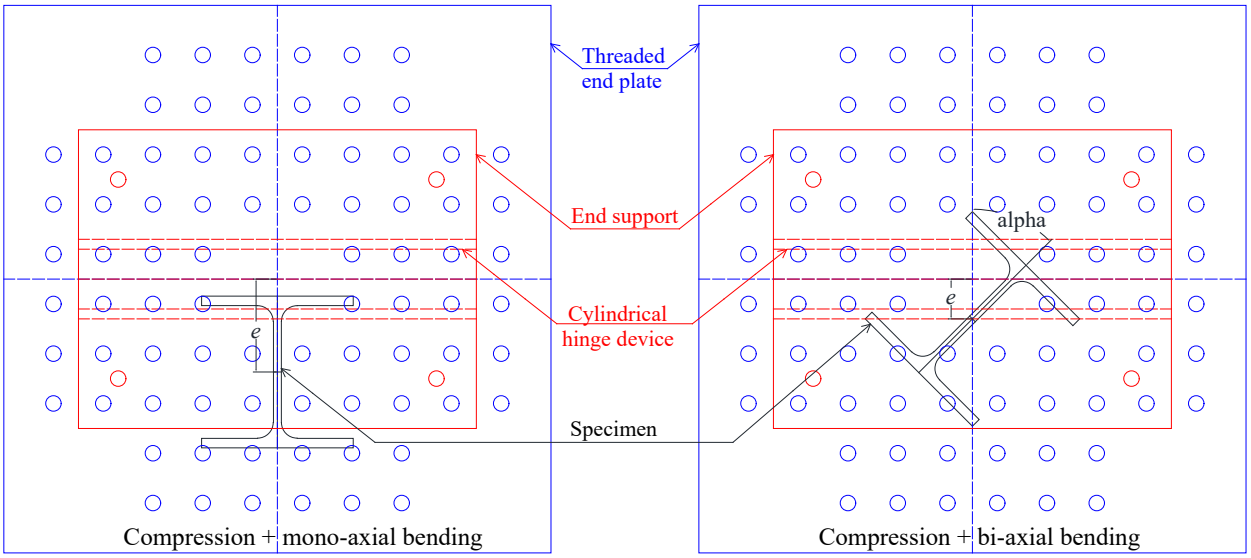


Figure 10: Schematic diagram showing position of member for the two load cases

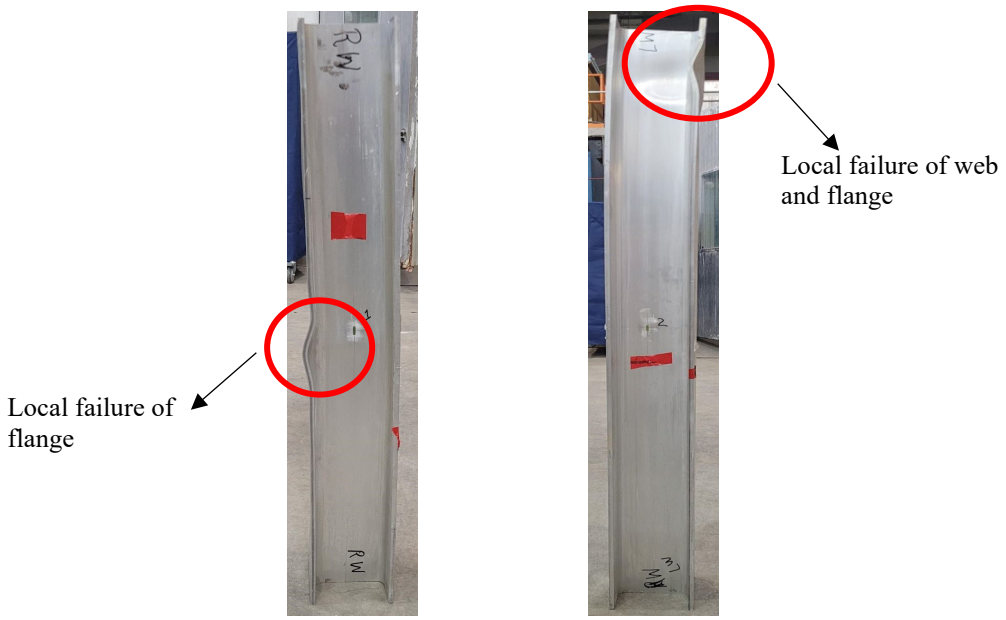


Figure 11: Failure modes for member specimens: (a) WF 6x7.61-3; (b) WF 6x7.61-4

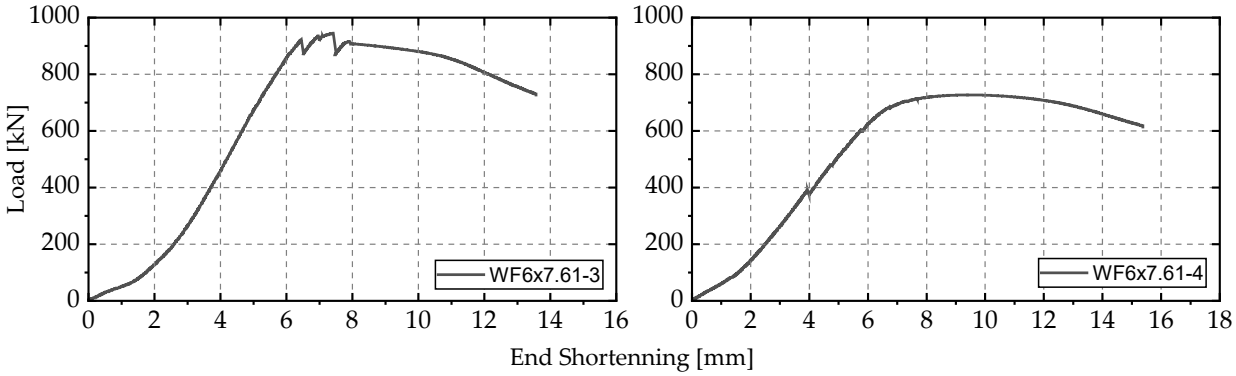


Figure 12: Load – Displacement curves for member specimens

Table 3: Peak loads and corresponding displacements, and comparison with Canadian Standard CSA S157

| Specimen | $N_{exp}$ [kN] | $\delta_{exp}$ [MPa] | $N_{CSA-S157}$ [kN] | Deviation from CSA S157 = $\frac{\lvert N_{exp}-N_{CSA-157}\rvert * 100}{N_{exp}}$ [%] |
|---|---|---|---|---|
| I6x3.92-1 | 603.50 | 3.15 | 460 | 24% |
| I6x3.92-2 | 605.50 | 3.30 | 460 | 24% |
| WF6x7.61-1 | 1241.45 | 5.35 | 859 | 31% |
| WF6x7.61-2 | 1220.15 | 4.20 | 859 | 30% |
| MEMBERS | | | | |
| WF6x7.61-3 | 944.96 | 7.4 | - | - |
| WF6x7.61-4 | 727.01 | 9.3 | - | - |

## 6. Conclusions and future work

This study focused on studying the local and member buckling behavior of extruded aluminum sections and members with I and H cross-sectional shapes. Accordingly, an experimental programme was carried out to study both local and global buckling of the above-mentioned specimens under pure compression for sections and under eccentric compression for members. The obtained experimental peak loads were compared to the resistance predictions from Canadian

standard CSA S157 for the short sections, and it was found that the Canadian standard provides conservative resistance predictions by 24 to 31%. It is therefore concluded that there is a need to come up with a better design methodology to improve economy and accuracy in designs. As a part of future studies, comparison of peak loads obtained from experimental series to resistance predictions from Canadian or other international standards will be examined, both at the section and member levels.

Besides, a numerical model within software Abaqus is currently under development; the latter will replicate the already-performed experimental tests to validate the numerical model. Consequently, a series of numerical parametric studies shall be performed, with varying loading conditions, cross-sectional shapes and slenderness for an in-depth study of buckling phenomena in I and H -shaped aluminum elements.

**Acknowledgement**
We would like to thank "Fonds de Recherche du Québec – NATURE ET TECHNOLOGIE (FRQNT) for funding this project. We also thank our industry funding partner MAADI Group Inc. for providing the test specimens.

**References**

Aluminum Association. (2020). "Aluminum design manual". *Aluminum Association*, *Washington, D.C, USA*.

Beaulieu, D. Marsh, C. (2006). "Design of Aluminum Structures" *Presses de l'aluminium: Québec, QC, Canada*

Canadian Standards Association. (2017). ″Strength Design in Aluminum″. *Canadian Standards Association: Toronto, ON, Canada CSA S157-17*

European Committee for Standardization. (2007). "Eurocode 9: Design of aluminium structures - Part 1-1: General structural rules". *Commission of the European Community, Brussels, Belgium*.

European standard EN ISO 377. (1997). European Committee for Standardization, Central Secratariat: rue de Stassart 36, B-1050 Brussels, ICS 77.040.10; 77.140.01.

Huang, Y., Young, B. (2014). "The art of cold-formed steel and aluminium alloy coupon tests." *In Proceedings of the 7th European Conference on Steel and Composite Structures*, Naples, Italy.

Liu, M., Zhang, L., Wang, P., Chang, Y. (2015). "Experimental investigation on local buckling behaviors of stiffened closed-section thin-walled aluminum alloy columns under compression." *Thin-Walled Structures* 94, 188–198. https://doi.org/10/f7mv44

ASTM—American Society for Testing and Materials. (2015). "Standard Specification for Aluminum-Alloy Permanent Mold Castings". *ASTM International: West Conshohocken*, PA, USA ASTM B108-15.

Wang, Y.Q., Wang, Z.X., Hu, X.G., Han, J.K., Xing, H.J. (2016). "Experimental study and parametric analysis on the stability behavior of 7A04 high-strength aluminum alloy angle columns under axial compression." *Thin-Walled Structures* 108, 305–320. https://doi.org/10.1016/j.tws.2016.08.029

Yuan, L., Zhang, Q., Ouyang, Y. (2022). "Experimental investigation and design method of the flexural buckling resistance of high-strength aluminum alloy H-columns" *Structures Elsevier*, pp. 1339–1349.

Zhang, Y., Wang, Y., Wang, Z., Bu, Y., Fan, S., Zheng, B. (2020). "Experimental investigation and numerical analysis of pin-ended extruded aluminium alloy unequal angle columns." *Engineering Structures* 215, 110694. https://doi.org/10.1016/j.engstruct.2020.110694